Journal of Materials Chemistry C

Tetrapyridine/triphenyltriazine-conjugated electron transporters for low- power-consumption, high-stability phosphorescent OLEDs

Journal:	*Journal of Materials Chemistry C*
Manuscript ID	TC-ART-11-2022-004647.R1
Article Type:	Paper
Date Submitted by the Author:	08-Feb-2023
Complete List of Authors:	Kawano, Tomoya; Yamagata Daigaku, Organic Device Engineering Sasabe, Hisahiro; Yamagata Daigaku, Organic Device Engineering Saito, Yu; Yamagata Daigaku, Organic Device Engineering Chen, Yuhui; Yamagata Daigaku, Organic Device Engineering Kori, Yuma; Yamagata Daigaku, Organic Device Engineering Nakamura, Takeru; Yamagata Daigaku, Organic Device Engineering Abe, Shoki; Yamagata Daigaku, Organic Device Engineering Maruyama, Tomohiro; Yamagata Daigaku, Organic Device Engineering Kido, Junji; Yamagata Daigaku

Tetrapyridine/triphenyltriazine-conjugated electron transporters for low-power-consumption, high-stability phosphorescent OLEDs

Tomoya Kawano[1], Hisahiro Sasabe[1,2,3], Yu Saito[1], Yuhui Chen[1], Yuma Kori[1], Takeru Nakamura[1], Shoki Abe[1], Tomohiro Maruyama[1], Junji Kido*[1,2,3]

[1]Department of Organic Materials Science, Yamagata University, 4-3-16 Jonan, Yonezawa, Yamagata 992-8510, Japan, [2]Research Center of Organic Electronics (ROEL), Yamagata University, 4-3-16 Jonan, Yonezawa, Yamagata 992-8510, Japan, and [3]Frontier Center for Organic Materials (FROM), Yamagata University, 4-3-16 Jonan, Yonezawa, Yamagata 992-8510, Japan

Academic titles: Prof. H. Sasabe, Mr. T. Kawano, Mr. Y. Saito, Mr. Y. Chen, Mr. Y. Kori, Mr. T. Nakamura, Mr. S. Abe, Mr. T. Maruyama, Prof. J. Kido

*Corresponding author
E-mail: h-sasabe@yz.yamagata-u.ac.jp

Keywords: organic light-emitting devices; tetrapyridine; electron-transporter; phosphorescence; long lifetime

Abstract: The electron transport layer (ETL) is one of the three primary layers for realizing low-power-consumption organic light-emitting devices (OLEDs). However, robust wide-energy-gap ETLs with high thermal and electrical stability have rarely been explored. In this study, we newly designed and developed a series of tetrapyridine/triphenyltriazine-conjugated ETLs, named **TnPyTRZ** derivatives (n = 2, 3, 4), to realize a low-power-consumption OLED with high operational stability. A green phosphorescent OLED based on **T3PyTRZ** simultaneously realized a low turn-on voltage (V_{on}) at 1 cd/m^2 of 2.18 V, a high external quantum efficiency of over 24%, a high power efficiency of over 115 lm/W, a long lifetime (LT_{50}) of 30000 h at a high brightness of 1000 cd/m^2. Even at 1000 cd/m^2, the driving voltage was only 2.88 V. This performance is among the best reported to date.

Introduction

Low-power-consumption organic light-emitting devices (OLEDs) are among the most attractive candidates for eco-friendly illumination light sources and displays.[1] To achieve low power consumption, a high external quantum efficiency (EQE) and low driving voltages must be simultaneously achieved at a practical luminance range of 1–5000 cd/m^2 for small-to-large-area display applications. In OLEDs, there are three primary layers: hole transport layer (HTL), emission layer (EML), and electron transport layer (ETL). Among them, the ETL significantly contributes to reducing the driving voltages owing to the much lower carrier injection and mobility compared with those of the HTL.[2] Among the wide-energy-gap ETLs that can be used for blue and green phosphorescent and/or thermally activated delayed fluorescence (TADF) OLEDs, oligopyridine derivatives, such as phenyl pyridine and terpyridine derivatives, exhibit promising performance.

As an early example, Tanaka and Kido reported pyrimidine/phenylpyridine-conjugated ETLs named **BnPyMPM** derivatives.[3] Among these, **B3PyMPM** derivatives have realized an energy efficient green phosphorescent OLED with a power efficiency of over 130 lm/W and an EQE of 30%. However, **BnPyMPM** derivatives exhibit poor stability in OLEDs. Xiao et al. developed a series of terpyridine-end-capped spirobifluorene ETLs, named **TPSF** derivatives.[4] These derivatives have an acceptor-donor-acceptor (A-D-A) structure to promote the stability of hole carriers, realizing a green phosphorescent OLED with an LT_{50} of 10000 cd/m^2 for over 100 h. Recently, Zhang et al. developed a spirobithioxanthene-based ETL called **T3PySS**.[5] **T3PySS** has a high triplet energy of 2.75 eV derived from its spiro-structure, an electron mobility of 10^{-4} cm^2/Vs, and a stable green phosphorescent OLED with LT_{90} at 2000 cd/m^2 for 1100 h. Recently, Sasabe and Kido reported a dibenzothiophen/terpyridine-conjugated ETL, named **snTPy**.[6] Among the three derivatives, **s4TPy** simultaneously realized a green phosphorescent OLED with a low turn-on voltage (V_{on}) of 2.8 V at 1 cd/m^2, a high EQE of 24%, and an LT_{50} of nearly 20000 h at 1000 cd/m^2. Zhang and Duan developed

phenylpyridine/anthracene-conjugated ETL named **DPPyA** realizing ultrahigh-efficinecy green phosphorescent OLEDs with a voltage under 3 V and a power efficiency of nearly 110 lm/W at a high luminance of 10000 cd/m^2.[7] However, the stability of the device was not reported. Recent reports on long lifetime ETLs based on oligopyridine derivatives are summarized in **Table S1**. As can be seen, previous ETLs such as **BnPyMPM**, **TPSF**, **snTPy**, **DPPyA** derivatives, partially realized 1) low voltage, 2) high EQE, and 3) long lifetime. However, none of them realized these key performances at the same time. A main challenge in the current ETLs is simultaneous realization of these key performances.

In this study, we newly designed and synthesized a series of tetrapyridine/triphenyltriazine-conjugated ETLs named **TnPyTRZ**. Among **TnPyTRZ** derivatives, a green phosphorescent OLED based on **T3PyTRZ** simultaneously realized a low turn-on voltage (V_{on}) at 1 cd/m^2 of 2.18 V, a high EQE of over 24%, a high power efficiency of over 115 lm/W, and a long lifetime of 30000 h at 1000 cd/m^2. Even at high brightness of 1000 cd/m^2, the driving voltage was only 2.88 V. These performances are among the best reported in the literature (**Table S1**).

Results and discussion

Molecular design, quantum chemical calculations, syntheses, and characterization

In our previous work, we developed a tetrapyridine-based ETL named **6,6'-BPy3TPy**.[8] It achieved comparable performances in terms of the efficiency in deep-red phosphorescent OLED to those of phenanthroline derivative **DPB**,[9] which is a conventional ETL that realizes high efficiency and long lifetime in phosphorescent and TADF OLEDs. From the perspective of chemical structure, the node of the lowest unoccupied molecular orbital (LUMO) of **6,6'-BPy3TPy** is located at the center of the molecule (**Figure S1**). **6,6'-BPy3TPy** is a dimer of the corresponding tetrapyridine, and the LUMO is symmetrically distributed on each tetrapyridine moieties, thus, the key component to exhibit the superior electron-transport property and realize promising performance in OLED can be attributed to the tetrapyridine moiety. Meanwhile,

tripheyltriazine is a well-known component for the hole-blocking layer (HBL) and/or ETL in long-lifetime OLEDs.[2,10] Inspired by these findings, we combined the tetrapyridine and triphenyltriazine moieties to design **TnPyTRZ** derivatives (n = 2–4) (**Figure 1**). Density functional theory (DFT) calculations were performed using Gaussian09 [11] to estimate the optoelectronic properties, such as the highest occupied molecular orbital (HOMO), LUMO, and E_T. The HOMO and LUMO levels increased depending on the position of the peripheral pyridine rings in the order of 2 > 3 > 4. This tendency is similar to that observed for other oligopyridine-based ETLs [2c, 3]. The E_T values were calculated to be greater than 2.85 eV, which is applicable for blue and green TADF and/or phosphorescent OLEDs. **TnPyTRZ** derivatives can be easily prepared on the gram scale by a two-step reaction, including the Kröhnke-type ring-closure reaction and Suzuki coupling reaction (see **Scheme S1** in SI). The precursor bromides and the final compounds were characterized by ^{1}H-NMR, ^{13}C-NMR, mass spectrometry, and elemental analyses (**Figure S2–10**). The final compounds were purified using silica gel column chromatography and train sublimation. The purity of the compounds was >99.5%, as evaluated via ultra-performance liquid chromatography.

Thermal and photophysical properties

The thermal properties, such as the 5% weight loss (T_{d5}), melting point (T_m), and glass transition temperatures (T_g), were investigated via thermogravimetric analysis (TGA) and differential scanning calorimetry (DSC) (**Figure S11–16**). **TnPyTRZ** derivatives exhibit high thermal stability, with T_{d5} values over 480 °C and T_m values over 275 °C. Among these derivatives, only **T2PyTRZ** exhibited a T_g value of 115 °C. **T3PyTRZ** and **T4PyTRZ** have high crystallinity. The effect of peripheral pyridine rings can be deduced from the T_m values because the structural differences among three derivatives are only the substitution positions of peripheral pyridine rings. The T_m values clearly increased in the order of 2 (279˚C) < 3 (304˚C) < 4 (321˚C) indicating the intermolecular interactions are increased in this order. Based on the

previous report on pyridine-containing ETLs, 3- and 4-pyridine derivatives can form multipule intermolecular hydrogen bonding interactions causing high crystallinity[3]. The triphenyltriazine moiety has large π-plane and easily forms π–π stacking[10] compared with other smaller pendant units such as dibenzothiophen[6] and fluorene[4]. Therefore, it can be considered that the crystallinity of **TnPyTRZ** (n = 3, 4) is high due to strong π-π stacking between triazine moieties and weak hydrogen bonding between peripheral pyridine rings. Note that three demensional structure in vacuum deposited film used in OLED is not same in the single crystal. The photophysical properties were then investigated. Ionization potential (I_p) was evaluated using photoelectron yield spectrometry. As predicted by the DFT calculations, **TnPyTRZ** exhibited different I_p values of –6.6 ~ –6.9 eV depending on the position of the peripheral pyridine rings, and the order was 2 > 3 > 4. The I_p values were much deeper than those of the phenanthroline-based ETL **nBPhen** (–6.3 eV).[12] The optical energy gap (E_g) was estimated from the UV-vis absorption spectra, and was determined as 3.4 eV (**Figure S17**). The electron affinity (E_a) was calculated using the I_p and E_g values, and different E_a values were observed depending on the peripheral pyridine rings. This suggests that the order of electron injection properties from the cathode aluminum metal is 4 > 3 > 2. Low-temperature PL spectra were measured in a dilute 2-methyltetrahydrofuran solution to determine the E_T value (**Figure S18–20**). All derivatives exhibited high E_T values of approximately 2.9 eV estimated from the onset of phosphorescence spectra.

OLED performances (I)

To validate the performance of **TnPyTRZ** as an ETL, we fabricated green phosphorescent OLEDs based on **Ir(ppy)$_3$** with the structure [ITO (100 nm)/polymer buffer [13] (20 nm)/**NPD** (10 nm)/**4DBFHPB** [14] (10 nm)/**mCBP** [15] doped with 12 wt.% **Ir(ppy)$_3$** (15 nm)/**DBF-TRZ** [16] (10 nm)/ETL : 20 wt.% **Liq** doped (40 nm)/**Liq** (1 nm)/Al (100 nm)]. **nBPhen** was used as a reference. The chemical structures of the materials used in this device are illustrated

in **Figure 2a**, and the energy diagram of the device is displayed in **Figure 2b**. **DBF-TRZ** was used as HBL to prolong the lifetime[14,17]. Although **DBF-TRZ** has a shallower I_p value compared with **TnPyTRZ**, however, there is a large energy difference of 0.4-0.6 eV between EML and **DBF-TRZ** to effectively block hole carriers. In addition, We used a mixed layer with **Liq** for ETL to reduce the crystallinity and enhance the stability[18]. The device performance is summarized in **Table 2**. **Figure 3a** shows the electroluminescence (EL) spectra, and all the devices exhibited green emission with a peak wavelength of 516 nm from **Ir(ppy)$_3$**, without any emission from neighboring materials. The current density–voltage (*J–V*) and luminance–voltage (*L–V*) characteristics are shown in **Figure 3b**. The turn-on voltage (V_{on}) was recorded to be very low (2.64–2.74 V). At a high brightness of 1000 cd/m^2, these devices exhibited low driving voltages in the range of 3.76–3.79 V, which are comparable to those of **nBPhen**-based devices. Higher EQE values of over 24% were recorded even at a high brightness of 1000 cd/m^2 compared to that of **nBPhen** (EQE = 18.6%) (**Figure 3c**). Subsequently, the stability at a constant current density of 25 mA/cm^2, which corresponds to a luminance of 12500–16000 cd/m^2, was tested. All ETLs exhibited better stability than **nBPhen**, and the LT_{50} values were recorded to be in the range of 120–155 h, which is equivalent to 13000–16000 h at 1000 cd/m^2 (**Figure 3d**). Photographs of the encapsulated OLEDs before and after the stability test were shown in **Figure S21**. The emission was observed to be remained uniform after the stability test without appearing black spots. Then, we made electron-only devices with the structure of [ITO/ETL (100 nm)/Liq (1 nm)/Al] (**Figure S22**). As a result, the current density of **TnPyTRZ** derivatives increased in the order of 2 < 3 < 4. This suggests that electron-transport property increased in this order. **nBPhen** showed similar current density to that in **T3PyTRZ**. In OLEDs, there was a large difference in efficiency roll-off, and the order of efficiency roll-off was 2 > 3 ≈ 4. This order is almost inversely correlated with the order of the current density. Thus, the reason for the large efficiency roll-off can be considered to the electron-transport property of **TnPyTRZ** derivatives. The stability of the final device was correlated with the order of EQE

values at high luminance region over 1000 cd/m^2. This means that carrier imbalance is the main factor for the stability. One of the possible reasons to decrease the stability is the hole leakage to ETL causing chemical degradation of ETL. Note that we measured the lifetime under the constrant current density of 25 mA/cm^2, which is corresponding to the luminance of approximately 15000 cd/m^2.

OLED performances (II)

Although the results obtained above are among the best for **Ir(ppy)$_3$**-based OLEDs, their performance can be improved in terms of driving voltages and lifetimes. In this device, we used **mCBP**, which has a much larger energy gap than **Ir(ppy)$_3$**, as the host material. To improve the performance of **Ir(ppy)$_3$**-based OLEDs, we changed the host material from **mCBP** to indorocarbazole-based **DIC-TRZ.**[19] It has a narrower E_g, where the I_p value is 0.2 eV shallower and the E_a value is 0.3 eV deeper than that of **mCBP**, expecting reduced driving voltages (**Figure 2b**). Moreover, the superior density of state overlaps with the HTL and HBL, where the energy differences such as ΔI_p and ΔE_a are in the range of 0.0–0.2 eV, resulting in increased carrier injection.[20] Among the ETLs, **T3PyTRZ** exhibited the best performance in **mCBP**-based OLEDs. Therefore, we investigated the effect of the host material using **T3PyTRZ** as the ETL. **Figure 4a** shows the EL spectra, and all the devices exhibited green emission with a peak wavelength of 519 nm from **Ir(ppy)$_3$**, without any emission from neighboring materials. Much improved *J–V* and *L–V* characteristics were obtained using **DIC-TRZ** as the host material (**Figure 4b**). The turn-on voltage was recorded to be low (2.18 V), which is 0.46 V lower than that of the **mCBP**-based device. At a high brightness of 1000 cd/m^2, **DIC-TRZ**-based device had a driving voltage of 2.88 V, which is 0.9 V lower compared with that of **mCBP**. In addition, EQE values of over 20% with reduced efficiency roll-off were recorded even at a high brightness of 10000 cd/m^2 (**Figure 4c**). The reduced driving voltages contribute to increasing the maximum power efficiency to 115 and 88 lm/W at 1000 cd/m^2. The

stability of **DIC-TRZ**-based device was significantly improved to an LT_{50} value of 251 h (**Figure 4d**), which is equivalent to over 30000 h at 1000 cd/m^2 when estimated using the well-known stretched exponential decay function (n = 1.75).[21]

Conclusions

We developed a new series of tetrapyridine-based ETLs, named **TnPyTRZ**, composed of tetrapyridine and triphenyltriazine moieties. Among these derivatives, only **T2PyTRZ** exhibited a T_g of 115 °C. However, **T3PyTRZ** and **T4PyTRZ** had high crystallinity induced by the synergistic effect of multiple weak hydrogen bonds and strong π–π stacking of the triphenyltriazine moiety. Regarding the optoelectronic properties, these ETLs have deeper I_p below –6.6 eV, E_a below –3.2 eV, and a high E_T of over 2.7 eV. The I_p and E_a values changed depending on the position of the peripheral pyridine rings and deepened in the order of 2 > 3 > 4, indicating superior electron injection properties. To validate the functions of **TnPyTRZ** as an ETL, we fabricated green phosphorescent OLEDs using **Ir(ppy)$_3$** as the emitter. The corresponding devices exhibited a high EQE of over 24%, V_{on} of 2.64 V, and high operational stability with an LT_{50} of over 13000 h at 1000 cd/m^2 when **mCBP** was used as the host material. To further reduce the driving voltages, we changed the host material from **mCBP** to **DIC-TRZ**, which had a significantly lower E_g value. As expected, the **DIC-TRZ**-based device exhibited much low V_{on} of 2.18 V, and 2.88 V at 1000 cd/m^2 with high EQE of nearly 23%, resulting in an increased power efficiency of 115 lm/W at maximum, and 88 lm/W at 1000 cd/m^2. Remarkably, the stability of the **DIC-TRZ**-based device was significantly enhanced to an LT_{50} of over 30000 h at 1000 cd/m^2. By using a combination of **TnPyTRZ** and **DIC-TRZ**, we successfully realized high-efficiency, low driving voltages, and long lifetimes. In other words, we developed low-power-consumption OLEDs with high operational stability at high brightness. We believe that this work will contribute to the development of next-generation low-power-consumption displays and illumination light sources.

Supporting Information

Supporting information is available.

Acknowledgements

We gratefully acknowledge partial financial support from the Center of Innovation (COI) Program of the Japan Science and Technology Agency (JST) and the subsidy program for the development of advanced research infrastructure from the Ministry of Education, Culture, Sports, Science, and Technology (MEXT). H.S. acknowledges the partial financial support from JSPS KAKENHI (20H02807) from the Japan Society for the Promotion of Science (JSPS).

References

[1] (a) C. Adachi, *Jpn. J. Appl. Phys.* **2014**, *53*, 060101; (b) Z. Yang, Z. Mao, Z. Xie, Y. Zhang, S. Liu, J. Zhao, J. Xu, Z. Chi, M. P. Aldred, *Chem. Soc. Rev.* **2017**, *46*, 915; (c) Y. Im, M. Kim, Y. J. Cho, J.-A Seo, K. S. Yook, J. Y. Lee, *Chem. Mater.* **2017**, *29*, 1946; (d) M. Y. Wong, E. Z.-Colman, *Adv. Mater.* **2017**, *29*, 1605444; (e) K. H. Kim, J. J. Kim, *Adv. Mater.*, **2018**, *30*, 1705600; (f) S. Scholz, D. Kondakov, B. Lüssem, and K. Leo, *Chem. Rev.,* **2015**, *115*, 8449; (g) G. Li, Z. Q. Zhu, Q. Chen, J. Li, *Org. Electron.*, **2019**, *69*, 135; (h) Y. Wang, J. H. Yun, L. Wang, J. Y. Lee, *Adv. Funct. Mater.*, **2021**, *31*, 2008332; (i) Y. Watanabe, H. Sasabe, J. Kido, *Bull. Chem. Soc. Jpn.* **2019**, *92*, 716; (j) S. S. Swayamprabha, D. K. Dubey, Shanawaz, R. A. K. Yadav, M. R. Nagar, A. Sharma, F.-C. Tung, J.-H. Jou, *Adv. Sci.* **2021**, *8*, 2002254.

[2] (a) A. P. Kulkarni, C. J. Tonzola, A. Babel, S. A. Jenekhe, *Chem. Mater.* **2004**, *16*, 4556; (b) G. Hughes, M. R. Bryce, *J. Mater. Chem.* **2005**, *15*, 94; (c) H. Sasabe, J. Kido, *Chem. Mater.* **2011**, *23*, 621; (d) L. Xiao, Z. Chen, B. Qu, J. Luo, S. Kong, Q. Gong, J. Kido, *Adv. Mater.* **2011**, *23*, 926; (e) D. Chen, S. -J. Su, Y. Cao, *J. Mater. Chem. C*, **2014**, *2*, 9565.

[3] (a) D. Tanaka, H. Sasabe, Y.-J. Li, S.-J. Su, T. Takeda, J. Kido, *Jpn. J. Appl. Phys.* **2007**, *46*, L10; (b) H. Sasabe, D. Tanaka, D. Yokoyama, T. Chiba, Y.-J. Pu, K.-i. Nakayama, M. Yokoyama, J. Kido, *Adv. Funct. Mater.* **2011**, *21*, 336; (c) D. Yokoyama, H. Sasabe, Y. Furukawa, C. Adachi, J. Kido, *Adv. Funct. Mater.* **2011**, *21*, 1375

[4] (a) M. Bian, D. Zhang, Y. Wang, Y-H. Chung, Y. Liu, H. Ting, L. Duan, Z. Chen, Z. Bian, Z. Liu, L. Xiao, *Adv. Funct. Mater.* **2018**, *28*, 1800429; (b) X. Guo, M. Bian, F. Lv, Y. Wang, Z. Zhao, Z. Bian, Z. Liu, B. Qu, L. Xiao, Z. Chen, *J. Mater. Chem. C*, **2019**, *7*, 11581; (c) X. Guo, Z. Tang, W. Yu, Y. Wang, Z. Zhao, J. Gu, Z. Liu, B. Qu, L. Xiao, Z. Chen, *Org. Electron.* **2021**, *89*, 106048; (d) M. Bian, Y. Wang, X. Guo, F. Lv, Z Chen, L. Duan, Z. Bian, Z. Liu, H. Geng, L. Xiao, *J. Mater. Chem. C,* **2018**, *6*, 10276.

[5] K. Duan, Y. Zhu, Z. Liu, D. Wang, C. Deng, S. Niu, T. Tsuboi, Q. Zhang, *Chem. Eng. J.* **2022**, *429*, 132215.

[6] T. Maruyama, H. Sasabe, Y. Watanabe, T. Owada, R. Yoshioka, Y. Saito, T. Kawano, J. Kido, *Chem. Lett.* **2021**, *50*, 534.

[7] D. Zhang, J. Qiao, D. Zhang, L. Duan, *Adv. Mater.* **2017**, *29*, 1702847.

[8] Y. Watanabe, D. Yokoyama, T. Koganezawa, H. Katagiri, T. Ito, S. Ohisa, T. Chiba, H. Sasabe, J. Kido, *Adv. Mater.* **2019**, *31*, 1808300.

[9] Y.-J. Pu, G. Nakata, H. Satoh, H. Sasabe, D. Yokoyama, J. Kido, *Adv. Mater.* **2012**, *24*, 1765.

[10] (a) L. S. Cui, S. B. Ruan, F. Bencheikh, R. Nagata, L. Zhang, K. Inada, H. Nakanotani, L. S. Liao, C. Adachi, *Nat. Commun.* **2017**, *8*, 2250. (b) M. Sarma, K.-T. Wong, *ACS Appl. Mater. Interf.* **2018**, *10*, 19279; (c) Y. Nagai, H. Sasabe, J. Takahashi, N. Onuma, T. Ito, S. Ohisa, J. Kido, *J. Mater. Chem. C* **2017**, *5*, 527; (d) H-F. Chen, S-J. Yang, Z-H. Tsai, W-Y. Hung, T-C. Wang, K.-T. Wong, *J. Mater. Chem.* **2009**, *19*, 8112; (e) K. Yamaguchi, T. Matsushima, A. S. D. Sandanayaka, Y. Homma, N. Uchida, C. Adachi, *Chem. Eur. J.* **2020**, *26*, 5598; (f) K. H. Choi, K. H. Lee, J. Y. Lee, T. Kim, *Adv. Opt. Mater.* **2019**, *7*, 1901374; (g) Y. Watanabe, H. Sasabe, D. Yokoyama, T. Beppu, H. Katagiri, Y.-J. Pu, J. Kido, *Adv. Opt. Mater.* **2015**, *3*, 769.

[11] *Gaussian 09*, Revision D.01, M. J. Frisch, G. W. Trucks, H. B. Schlegel, G. E. Scuseria, M. A. Robb, J. R. Cheeseman, G. Scalmani, V. Barone, B. Mennucci, G. A. Petersson, H. Nakatsuji, M. Caricato, X. Li, H. P. Hratchian, A. F. Izmaylov, J. Bloino, G. Zheng, J. L. Sonnenberg, M. Hada, M. Ehara, K. Toyota, R. Fukuda, J. Hasegawa, M. Ishida, T. Nakajima, Y. Honda, O. Kitao, H. Nakai, T. Vreven, J. A. Montgomery, Jr., J. E. Peralta, F. Ogliaro, M. Bearpark, J. J. Heyd, E. Brothers, K. N. Kudin, V. N. Staroverov, R. Kobayashi, J. Normand, K. Raghavachari, A. Rendell, J. C. Burant, S. S. Iyengar, J. Tomasi, M. Cossi, N. Rega, J. M. Millam, M. Klene, J. E. Knox, J. B. Cross, V. Bakken,

C. Adamo, J. Jaramillo, R. Gomperts, R. E. Stratmann, O. Yazyev, A. J. Austin, R. Cammi, C. Pomelli, J. W. Ochterski, R. L. Martin, K. Morokuma, V. G. Zakrzewski, G. A. Voth, P. Salvador, J. J. Dannenberg, S. Dapprich, A. D. Daniels, Ö. Farkas, J. B. Foresman, J. V. Ortiz, J. Cioslowski, and D. J. Fox, Gaussian, Inc., Wallingford CT, 2013.

[12] (a) Z. Wang, M. Li, L. Gan, X. Cai, B. Li, D. Chen, S.-J. Su, *Adv. Sci.* **2019**, *6*, 1802246; (b) H. Tsuneyama, H. Sasabe, Y. Saito, T. Noda, D. Saito, J. Kido, *J. Mater. Chem. C* **2022**, *10*, 2073.

[13] J. Kido, G. Harada, M. Komada, H. Shionoya, K. Nagai, *ACS. Synp. Ser.* **1997**, *672*, 381.

[14] (a) T. Kamata, H. Sasabe, M. Igarashi, J. Kido, *Chem. Eur. J.* **2018**, *24*, 4590; (b) T. Kamata, H. Sasabe, N. Ito, Y. Sukegawa, A. Arai, T. Chiba, D. Yokoyama, J. Kido, *J. Mater. Chem. C* **2020**, *8*, 7200.

[15] P. Schrögel, N. Langer, C. Shildknecht, G. Wagenblast, C. Lennartz, P. Strohriegl, *Org. Electron.* **2011**, *12*, 2047.

[16] T. Ito, H. Sasabe, Y. Nagai, Y. Watanabe, N. Onuma, J. Kido, *Chem. Eur. J.* **2019**, *25*, 7308.

[17] N. Nagamura, H. Sasabe, H. Sato, T. Kamata, N. Ito, S. Abe, S. Araki, Y. Sukegawa, D. Yokoyama, H. Kaji, J. Kido, *J. Mater. Chem. C* **2022**, *10*, 8694.

[18] (a) H. Tsuneyama, H. Sasabe, Y. Saito, T. Noda, D. Saito, J. Kido, *J. Mater. Chem. C* **2022**, 10, 2073; (b) D. P.-K. Tsang, T. Matsushima, C. Adachi, *Sci. Rep.* **2016**, *6*, 22463; (c) J. Endo, T. Matsumoto and J. Kido, *Jpn. J. Appl. Phys. Part 2*, **2002**, *41*, L800; (d) C. Schmitz, H.-W. Schmidt, M. Thelakkat, *Chem. Mater.* **2000**, *12*, 3012.

[19] D. Zhang, L. Duan, C. Li, Y. Li, H. Li, D. Zhang, Y. Qiu, *Adv. Mater.* **2014**, *26*, 5050.

[20] T. Matsushima, K. Goushi, C. Adachi, *Chem. Phys. Lett.* **2007**, *435*, 327.

[21] D. Zhang, M. Cai, Y. Zhang, D. Zhang, L. Duan, *Mater. Horiz.* **2016**, *3*, 145.

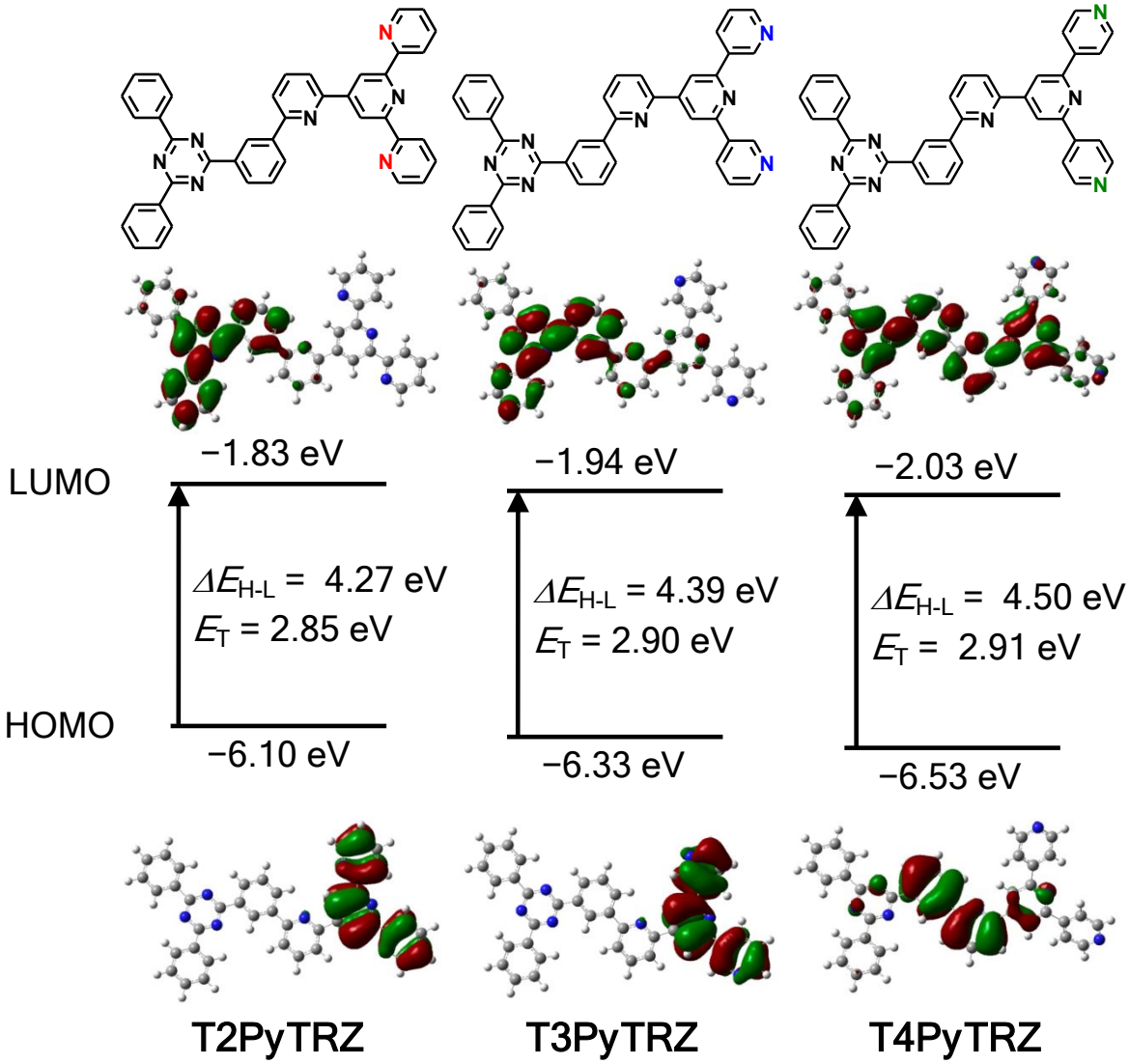

Figure 1. Chemical structure of **TnPyTRZ** derivatives; HOMO and LUMO distributions and energy levels; HOMO-LUMO energy differences (ΔE_{H-L}); and the lowest triplet energy (E_T).

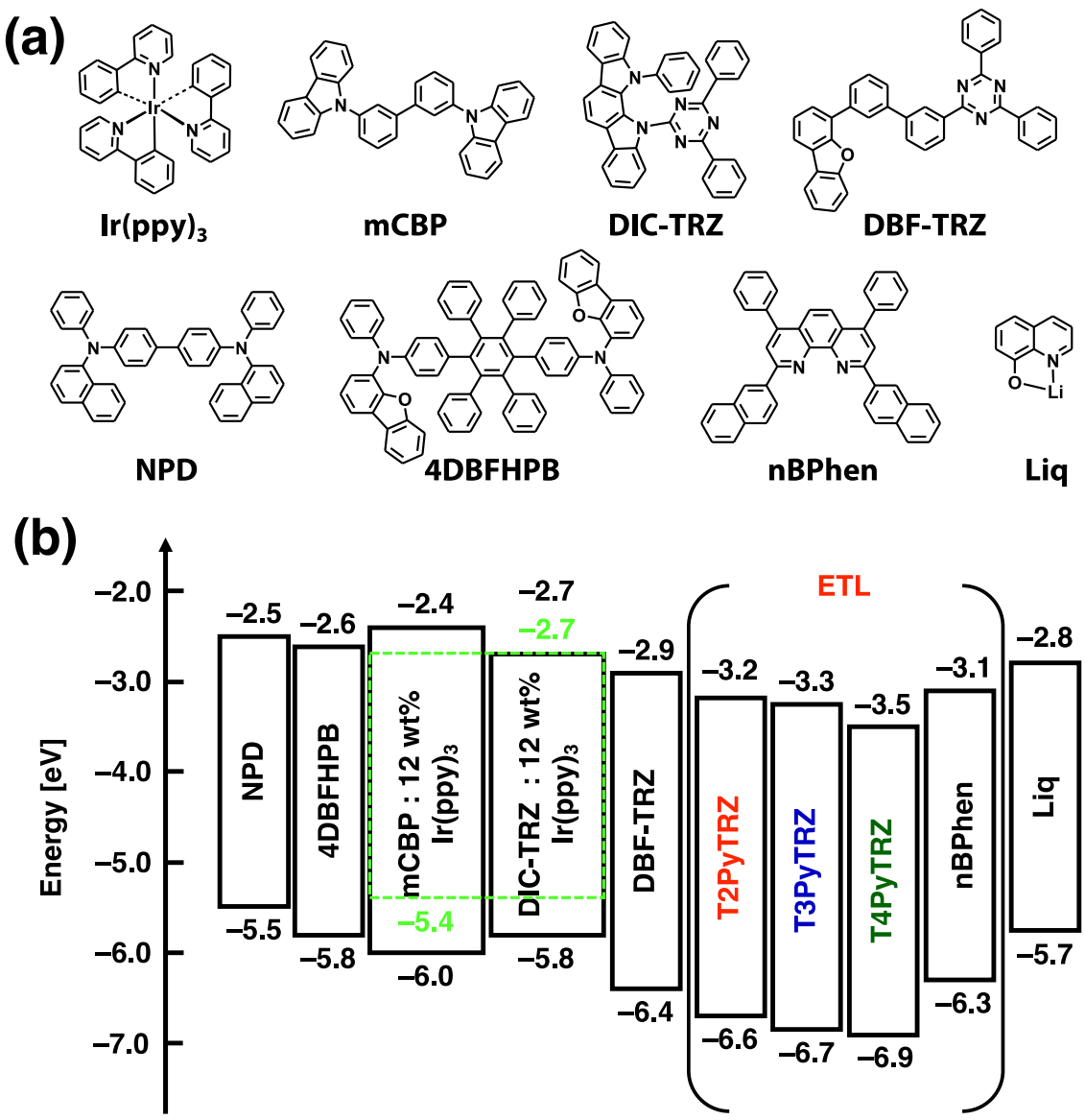

Figure 2. (a) Chemical structures of the materials used in OLEDs. (b) Energy diagram of the OLED.

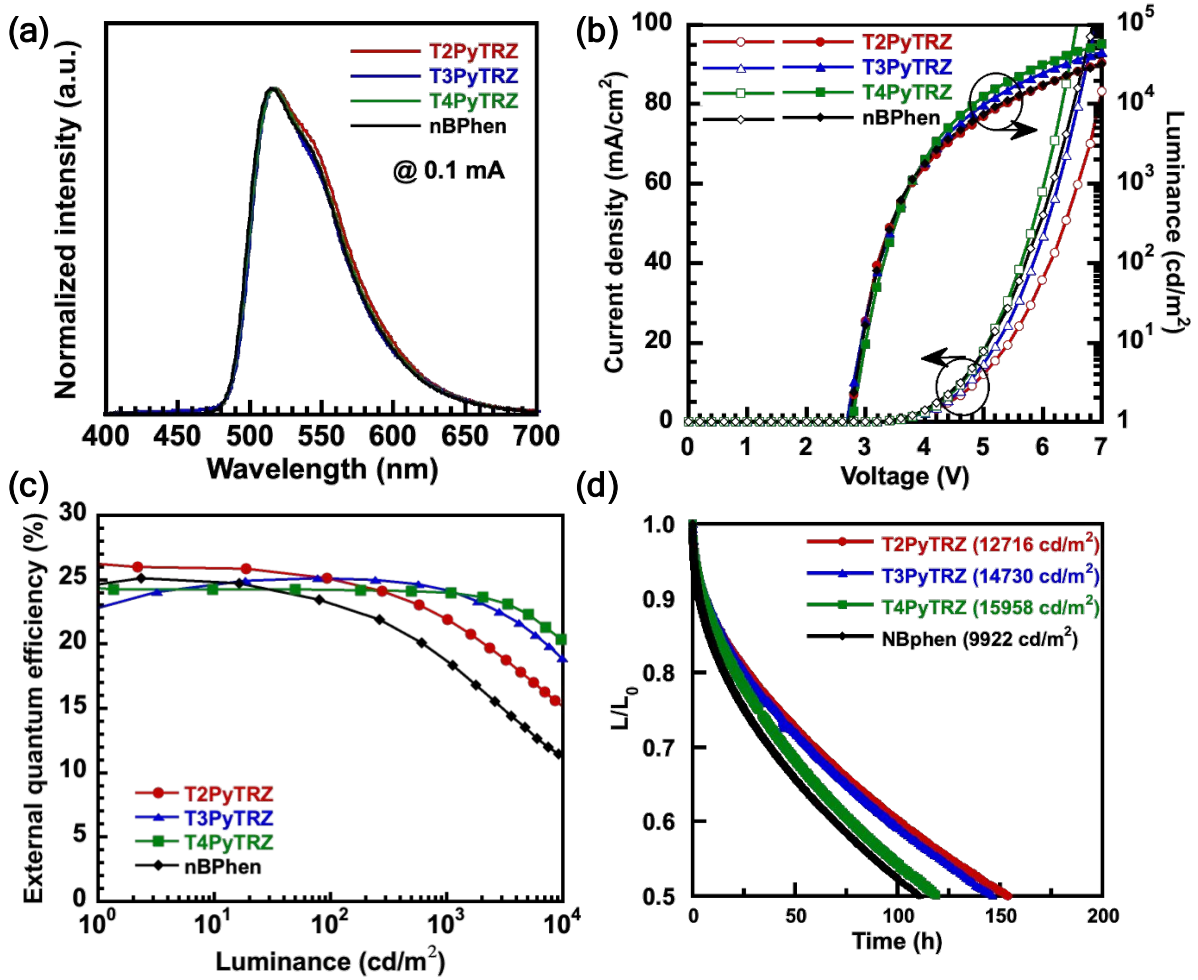

Figure 3. Device performance of green phosphorescent OLEDs based on **mCBP** as the host material: a) EL spectra. b) *J–V–L* characteristics. c) *EQE–L* characteristics. d) Operational lifetime at 25 mA cm^{-2}.

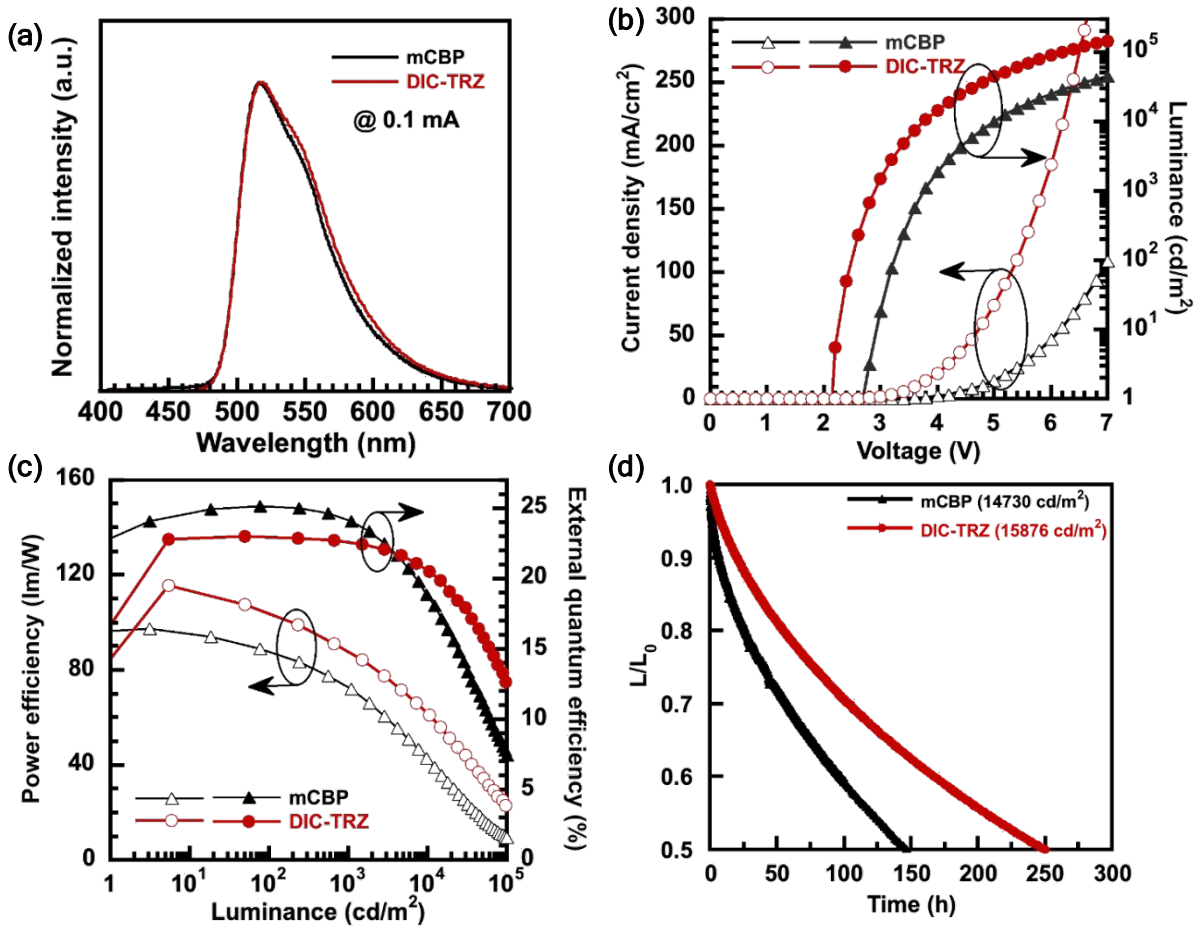

Figure 4. Device performance of green phosphorescent OLEDs based on **DIC-TRZ** as the host material: a) EL spectra. b) *J–V–L* characteristics. c) *PE–EQE–L* characteristics. d) Operational lifetime at 25 mA cm^{-2}.

Table 1. Thermal and optical properties.

Compound	MW	T_g[a]/T_m[a]/T_{d5}[b] (ºC)	HOMO[c]/LUMO[c]/E_T[d] (eV)	I_p[e]/E_g[f]/E_a[g]/E_T[h] (eV)
T2PyTRZ	617.7	115/279/485	–6.10/–1.83/2.85	–6.6/3.4/–3.2/2.87
T3PyTRZ	617.7	n.d./304/481	–6.33/–1.94/2.90	–6.7/3.4/–3.3/2.90
T4PyTRZ	617.7	n.d./321/488	–6.53/–2.03/2.91	–6.9/3.4/–3.5/2.92

[a]T_g and T_m values were determined using DSC. [b]T_{d5} was determined by TGA. [c,d]Calculated at the B3LYP/ 6-31G(d)// B3LYP 6-31G(d) level. [d]Calculated triplet energies. [e]I_p was determined using photoelectron yield spectroscopy. [f]E_g was considered as the point at which the normalized absorption spectra intersected. [g]The value of E_a was calculated using I_p and E_g. [h]E_T was estimated from the onset of the phosphorescent spectra at 80 K.

Table 2. Summary of OLED performance.

Host	ETL	V_{on}[a] (V)	$V_{100}/CE_{100}/PE_{100}/EQE_{100}$[b] (V/cd A^{-1}/lm W^{-1}/%)	$V_{1000}/CE_{1000}/PE_{1000}/EQE_{1000}$[b] (V/cd A^{-1}/lm W^{-1}/%)	LT_{50} at 1000 cd m^{-2} (h)[c]
mCBP	**T2PyTRZ**	2.68	3.21/90.4/88.6/25.0	3.79/79.0/65.5/21.9	13272
	T3PyTRZ	2.64	3.23/90.5/88.1/25.1	3.76/87.2/72.8/24.2	16281
	T4PyTRZ	2.74	3.28/87.3/83.7/24.2	3.77/86.6/72.2/24.0	15290
	nBPhen	2.68	3.24/82.2/79.7/23.2	3.77/66.4/55.6/18.6	6157
DIC-TRZ	**T3PyTRZ**	2.18	2.45/81.9/104.9/22.9	2.88/80.6/88.0/22.5	31662

[a] Turn-on voltage at 1 cd m^{-2}, [b]voltage (*V*), current efficiency (*CE)*, power efficiency (*PE*), and external quantum efficiency (*EQE*) at 100 cd m^{-2}, [c]*V, CE*, *PE*, and *EQE* at 1000 cd m^{-2}. [c]Operation lifetime at 50% (LT_{50}) at 1000 cd m^{-2}.